Itaconic acid-modified layered double hydroxide as a novel adsorbent for effective removal of Congo red from aqueous solutions

Mohammad Dinari (dinari@iut.ac.ir)
Isfahan University of Technology https://orcid.org/0000-0001-5291-7142
Shirin Shabani
Isfahan University of Technology

Research Article

Keywords: Cu-Ca-Al/NO3-based layered double hydroxide, Itaconic acid, Adsorption, Congo red, Kinetic and isotherm

Posted Date: March 22nd, 2021

DOI: https://doi.org/10.21203/rs.3.rs-345643/v1

Itaconic acid-modified layered double hydroxide as a novel adsorbent for effective removal of Congo red from aqueous solutions

Mohammad Dinari[*a] and Shirin Shabani [b]

[a] *Department of Chemistry, Isfahan University of Technology, Isfahan 84156–83111, Iran*

[a] *Chemistry group, Pardis College, Isfahan University of Technology, Isfahan 84156-83111, I.R. Iran*

[*]Corresponding authors:

Mohammad Dinari, Department of Chemistry, Isfahan University of Technology, Isfahan 84156-83111, Iran

E-mail: dinari@iut.ac.ir

Abstract

Herein, we report the synthesis of Cu-Ca-Al/NO_3-based layered double hydroxide through co-precipitation methodology. The prepared layered double hydroxide was then modified with itaconic acid. The physicochemical properties of the prepared materials were studied using Fourier transform-infrared spectroscopy, scanning electron microscopy, X-ray diffraction analysis, thermogravimetric analysis, and nitrogen adsorption/desorption technique. The prepared materials were then applied as novel adsorbents for the removal of Congo red as a model of an anionic dye from aqueous media. To reach maximum adsorption, the effect of parameters including sample solution pH, adsorbent amount, contact time, and initial concentration of Congo red on the adsorption process was investigated. Kinetic studies were also conducted to study the mechanism of adsorption. In this regard, the kinetic models of pseudo-first-order, pseudo-second-order, Elovich, and intra-particle diffusion were studied. The results showed that the adsorption of Congo red onto Cu-Ca-Al-LDH and LDH-ITA adsorbents followed the pseudo-second-order kinetic model. To evaluate the equilibrium adsorption data, different isotherms including Langmuir, Freundlich, and Dubinin-Radushkevich were also applied. The data revealed that the Freundlich isotherm provided the best fit with the equilibrium data of both adsorbents. Maximum adsorption capacities of 81 and 84 mg g^{-1} were obtained using Cu-Ca-Al-LDH and LDH-ITA adsorbents, respectively.

Keywords: Cu-Ca-Al/NO_3-based layered double hydroxide; Itaconic acid; Adsorption; Congo red; Kinetic and isotherm

1. Introduction

As a growing trend, nanotechnology has attracted huge interest among scientists in various scientific fields such as catalysis [1-3], energy conversion and storage [4], sample preparation [5-8], and adsorption [9-15]. The great interest in the field of nanotechnology arises from the extraordinary physical, chemical, thermal, and mechanical characteristics of nanomaterials in comparison with large-size particles. In general, nano-sized materials exhibited high specific surface area, tailorable structure, thermal stability, high chemical and mechanical resistance, and easiness in functionalization. As a subgroup of inorganic layered nanomaterials, layered double hydroxides (LDHs) are ionic lamellar mixed hydroxides that consisted of positively charged main layers and an interlayer region with charge-compensating anions undergoing anion-exchange chemistry [16, 17]. They are generally demonstrated with a stoichiometry of $[M^{2+}_{1-x}M^{3+}_{x}(OH)_2]^{x+}(A^{n-})_{x/n}.mH_2O$ [18, 19]. In this formula, M^{2+} and M^{3+} represent divalent and trivalent metals of the layers, respectively, and A^{n-} is charge balancing anion in the interlayer region which can be readily replaced. Owing to their fantastic properties, nowadays LDHs with different compositions have received remarkable attention from academia and industry. They are exhibited important properties such as ion exchange capability, acid-base properties, and adsorption capacity. They are also low-cost materials and their properties can be easily tailored. The use of these materials in drug delivery [20], catalysis [21], energy conversion and storage [22], environmental remediation [23, 24], and sample preparation [25, 26] have been reported.

Despite the unique characteristics of LDHs, various functionalization strategies have been reported for the modification of LDHs to increase their performance and applications. Considering the surface properties of LDHs, they are easily agglomerated, usually incompatible with organic substances, and have low efficiency for specific applications. LDHs functionalization can drastically improve their performance and properties. Until now,

various functionalization strategies have been used for the modification of LDHs. Some common functionalization strategies included intercalation, hybrid assembly, surface modification, size and morphology regulation, layer composition tuning, and defect introduction which are discussed in detail in a reported review by Laipan et al [27].

As an important environmental concern in both developing and industrial countries, the lack of clean water due to the disposal of various toxic compounds into the environment caused drastic concerns about the creature's health. As an unpleasant result of the industrialization process, water pollution is an international problem, and nowadays scientists, and policymakers are beginning to take more notice of this vital problem to find a suitable solution. Among the well-known pollutants, synthetic organic dyes are one of the important groups of water pollutants. The release of these contaminants is an increasing and serious global challenge from the environmental point of view. These relatively complex organic molecules are widely used in different industries such as leather tanning, food processing, paper making, cosmetics, textile, and plastics. As a water-soluble member of synthetic dyes, Congo red is used in a huge quantity in textile and biochemistry based industries [28]. It is a benzidine-based anionic dye that was discovered by Paul Bottinger in 1883. Generally, benzidine-based dyes are toxic and highly carcinogenic. Congo red is known to metabolize to benzidine, which is a carcinogen and mutagen compound for humans. Due to the high toxicity and carcinogenicity of Congo red, its use is banned in many countries [29].

Until now, various decontamination techniques including biological, chemical, and physical treatments have been adopted to remove toxic compounds especially synthetic organic dyes from environmental media in both industrial and municipal wastewaters [30]. In this regard, the application of membrane separation, adsorption, chemical oxidation, chemical coagulation, biological degradation, etc. is reported [15]. Among the treatment techniques,

the adsorption strategy provided a simple, low cost, and relatively fast methodology with high efficiency. This conventional strategy is used in advanced wastewater treatment due to its ease of operation, and flexibility in adsorbent design. This method also produces no harmful by-products and prevents sludge formation during the removal process [15]. Until now, various synthetic and natural adsorbents have been used for the adsorption of organic dyes which is discussed in some useful review reports [31-33]. Notably, developing adsorbents with improved characteristics to be used for the adsorption process is an ongoing trend.

Herein, we present the synthesis and characterization of a novel adsorbent of itaconic acid-modified Cu-Ca-Al layered double hydroxide for adsorption purposes. The Cu-Ca-Al layered double hydroxide was synthesized at first and then modified with itaconic acid through a simple approach. To study the applicability of the prepared materials for adsorption purposes, Congo red as an anionic dye was selected to be removed from the aqueous solution. Kinetic studies were also conducted for the prepared materials. To the best of our knowledge, this is the first report to study the potential application of itaconic acid-modified Cu-Ca-Al layered double hydroxide for adsorption purposes.

2. Experimental section

2.1. Materials and methods

Aluminum nitrate nonahydrate ($Al(NO_3)_3.9H_2O$, ≥98.0%), calcium nitrate tetrahydrate ($Ca(NO_3)_2.4H_2O$, ≥99.0%), copper(II) nitrate trihydrate ($Cu(NO_3)_2.3H_2O$, ≥99.0%), sodium carbonate (Na_2CO_3), sodium hydroxide (NaOH), and itaconic acid ($C_5H_6O_4$) were purchased from Sigma-Aldrich. Acetic acid (99.5%) and *ortho*-phosphoric acid (85%) were obtained from Merck (Darmstadt, Germany). The stock standard solution of Congo red (2000 mg L^{-1})

was prepared in water. Working standard solutions were prepared daily by diluting the stock solution. Deionized water was prepared by a lab-made water purification system.

2.2. Apparatus

A double beam UV–Vis spectrophotometer (UV-1601 Shimadzu, Japan) was applied for the determination of dye concentration in the sample solutions at the wavelength of 499 nm. The XRD data were recorded with the help of a Rigaku-DMax 2500 diffractometer (Japanese science and science company, Tokyo, Japan) with Cu K_α radiation at a wavelength of 1.540 Å and the generator working at 40 kV. Diffractograms were recorded between 2θ of 5-70°. The FT-IR spectra were recorded on a Jasco-FT-IR-350 (Tokyo, Japan) spectrometer with a wavenumber range from 400 to 4400 cm^{-1}, using the KBr pellet technique. Scanning electron microscopy (SEM) was performed on a JSM-6510 Series scanning electron microscope (JEOL, Tokyo, Japan). Nitrogen adsorption/desorption analysis was performed using a Belsorp-mini II (BEL Japan Inc., Osaka, Japan) at the temperature of 77 K. Thermogravimetric analysis was performed on an STA 503 *(*Bahr GmbH*,* Hullhorst*,* Germany*)* analyzer, at a heating rate of 10 ºC min^{-1} from room temperature to 800 ºC under an inert atmosphere.

2.3. Synthesis of Cu-Ca-Al-LDH

The Cu-Ca-Al-LDH was prepared according to the following procedure. At first, 976 mg of $Cu(NO_3)_2 \cdot 3H_2O$ (4 mmol), 954 mg of $Ca(NO_3)_2.4H_2O$ (4 mmol), and 1.532 g of $Al(NO_3)_3 \cdot 9H_2O$ (4 mmol) were dissolved into 100 mL of deionized water. In another container, 100 mL of an aqueous alkaline solution containing 150 mmol L^{-1} of NaOH and 50 mmol L^{-1} of Na_2CO_3 was prepared. Then, the two prepared solutions were slowly added to a 500 mL round bottom glass flask. The pH of the solution was kept between 10 and 11 during

the addition. After the addition, the mixture was stirred at room temperature for 60 min. Then, the temperature of the solution was enhanced to 60 °C and maintained for 18 h. Afterward, the slurry was cooled and filtered. The prepared material (Cu-Ca-Al-LDH) was washed several times with deionized water and dried in an oven at 85 °C.

2.4. Synthesis of LDH-ITA

For the preparation of LDH-ITA, 976 mg of $Cu(NO_3)_2 \cdot 3H_2O$ (4 mmol), 954 mg of $Ca(NO_3)_2.4H_2O$ (4 mmol), and 1.532 g of $Al(NO_3)_3 \cdot 9H_2O$ (4 mmol) were dissolved into 100 mL of deionized water. Then, 100 mL of an aqueous alkaline solution containing 150 mmol L^{-1} of NaOH and 50 mmol L^{-1} of Na_2CO_3 was prepared. The two prepared solutions were then slowly added to a 500 mL round bottom flask at room temperature (the pH of the solution was kept in the range of 10- 11). The mixture was stirred for 60 min, heated to 60 °C, and then, 50 mL of water containing 2.5 g of itaconic acid was poured into the round bottom flask and stirred for 60 min. The mixture was maintained at this step for 18 h without stirring. The obtained slurry was filtered, washed with deionized water, and dried at 80 °C.

2.5. Adsorption experiments

The batch adsorption experiments were conducted to study the adsorption behavior of Congo red onto the prepared adsorbents. For the experiments, 5 mL of an aqueous solution of Congo red (with the desired concentration) was poured into a 25 mL Erlenmeyer flask containing the accurately weighed amount of adsorbent. The adsorption was carried out in a water-bath shaker (298 K) at a shaking speed of 220 rpm for a specific period. After separation of the adsorbent from the solution, the concentration of Congo red in the solution was determined with the help of the UV–Vis spectrophotometer at 499 nm. All the samples

were filtered through filter papers before analysis. The removal efficiency was calculated using the following equation (Eq. 1):

$$RE\ (\%) = \frac{C_i - C_e}{C_i} \times 100 \qquad (1)$$

In this equation, C_i and C_e are the initial and equilibrium concentration of Congo red in the solution (mg L^{-1}), respectively. The adsorption capacity (q_e, mg g^{-1}) was computed according to the following equation (Eq. 2):

$$q_e = \left(\frac{C_i - C_e}{W}\right) \times V \qquad (2)$$

In this equation, W is the adsorbent amount (mg) and V is the solution volume (mL).

3. Results and discussion

3.1. Synthesis and characterization of the materials

In this study, Cu-Ca-Al-LDH was prepared in a simple strategy. For the modification of the prepared LDH, itaconic acid was applied. Due to their ability to establish a hydrogen bond between surface hydroxyl groups and functional groups of organic dyes, as well as their ion exchange ability, Cu-Ca-Al-LDH and LDH-ITA can be used as adsorbents to remove organic dyes from aqueous media. Scheme 1 reveals the structure of these materials and possible interactions during adsorption of Congo red by them form the aqueous solution.

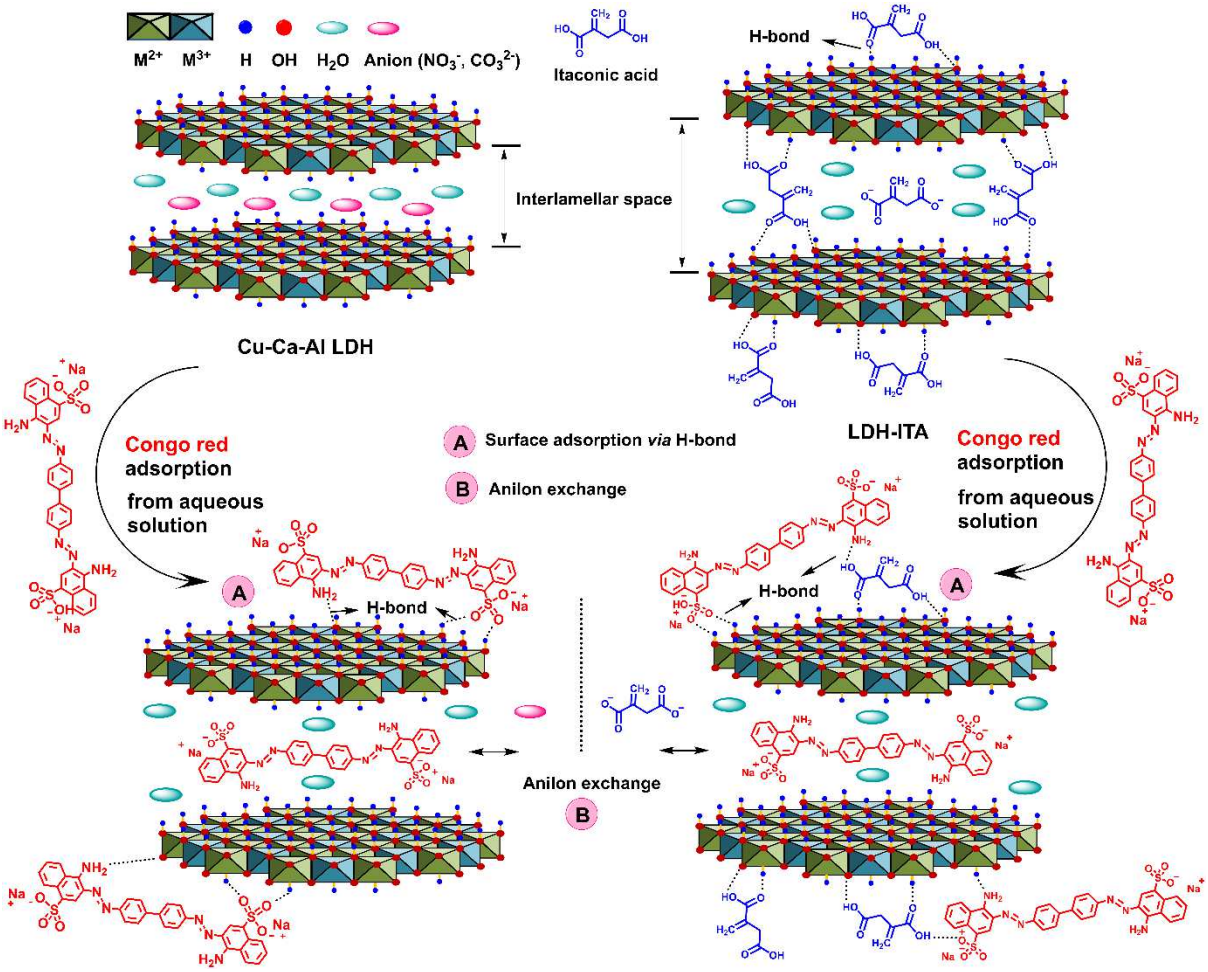

187

188 **Scheme 1** The schematic representation for structure of Cu-Ca-Al-LDH and LDH-ITA and

189 their application for adsorption of Congo red from the aqueous solutions.

190

191 The structure of the prepared materials was further studied using various

192 characterization techniques including FT-IR spectroscopy, X-ray diffraction (XRD), scanning

193 electron microscopy (SEM), N_2 adsorption/desorption, and thermogravimetric analysis

194 (TGA).

195 The FT-IR spectra of the prepared Cu-Ca-Al-LDH and LDH-ITA are shown in Fig. 1.

196 In the case of Cu-Ca-Al-LDH, the broadband located at 3435 cm^{-1} is associated with the

197 stretching vibration of O-H groups in the brucite-like layer and interlayer molecules. The

198 weak band located at around 1633 cm^{-1} is related to the bending vibration of interlayer water

199 molecules [34]. The band at 1421 cm^{-1} can be assigned to the characteristic vibration mode of

200 NO_3^- anions in the interlayer of the prepared Cu-Ca-Al-LDH. A series of complicated bands
201 in the range of 400-1000 cm^{-1} (such as 876, 712, 604, 515, 445 cm^{-1}, etc.) can be attributed to
202 the vibrational modes of the lattice resulting from M–O, O–M–O, and M–O–M bonds in
203 which the M represents Cu, Ca or Al [35]. In the case of modified LDH-ITA, the broadband
204 related to the stretching vibration of hydroxyl groups and water molecules in the interlayer
205 space can be seen at 3473 cm^{-1}. The band at 1421 cm^{-1} disappeared in the case of LDH-ITA,
206 indicating that most of the NO_3^- ions were replaced by itaconic acid anions. An absorption
207 band at 1384 cm^{-1} indicated the presence of some carboxylate anions in the modified
208 hydrotalcite structure. The bands located at 1646 cm^{-1} and 1431 cm^{-1} are related to the
209 absorption bands of the carboxylic ions (asymmetric and symmetric stretching absorptions).
210 The band at 1565 cm^{-1} is related to the C=C stretching vibration [36, 37]. These bands
211 indicated the intercalation of itaconic acid.

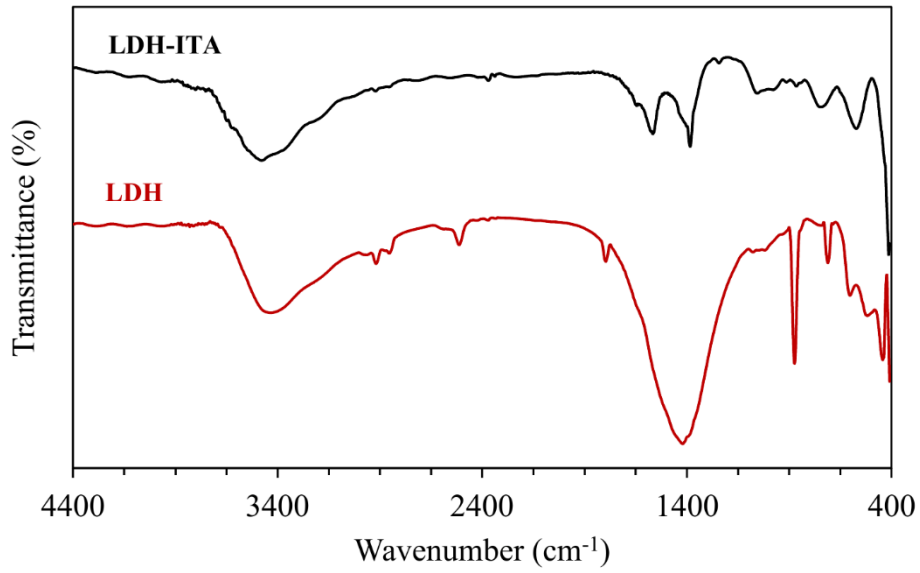

212

213 **Figure 1.** FT-IR spectra of the Cu-Ca-Al-LDH and LDH-ITA**.**

214 The XRD patterns of the prepared Cu-Ca-Al-LDH and LDH-ITA are shown in Fig. 2a.
215 In the case of Cu-Ca-Al-LDH, it exhibited characteristic peaks located at 2θ = 23.1°, 29.5°,
216 35.6°, 38.6°, 39.5°, 43.1°, 47.5°, 48.5°, etc. which is in accordance with previous reports
217 [38]. In this regard, the peaks at 35.6° and 38.6° correspond to CuO. The presence of

characteristic peaks related to $CaCO_3$ (23.4°, 29.5°, 36.9°, 39.5°, 43.1°, 47.5°, and 48.5°) is detected in the XRD pattern, which is in agreement with the previous reports on the synthesis of Ca–Al LDHs [39, 40]. In the LDH-ITA, some diffraction peaks disappeared or weakened. In contrast, some diffraction peaks became stronger or new peaks appeared. These observations combined with the earlier FTIR analyses indicated that itaconic acid was incorporated into the Cu-Ca-Al-LDH structure.

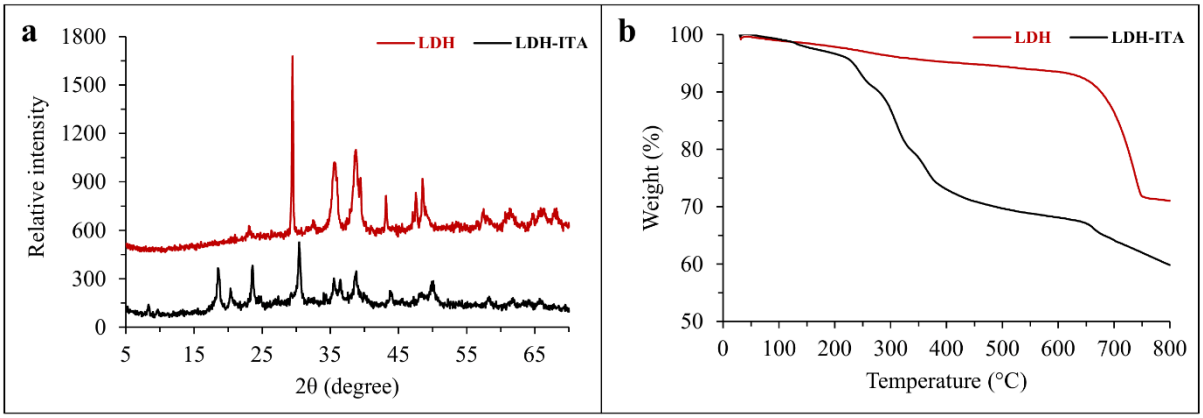

Figure 2. The XRD patterns (a) and the TGA thermograms (b) of the prepared Cu-Ca-Al-LDH and LDH-ITA.

The TGA curves of the prepared Cu-Ca-Al-LDH and LDH-ITA are shown in Fig. 2b. In the case of Cu-Ca-Al-LDH, a mass loss between 30 to 235 °C (about 2.7%) is mainly due to the removal of physically-adsorbed and interlayered water [36]. Another mass loss occurred between 235 to 580 °C (about 3.7%) which may be attributed to the decomposition of the lamina –OH groups. In this stage, the layered structure of the Cu-Ca-Al-LDH was gradually degraded. A final mass loss occurred in the range of 580 to 800 °C (about 22.6%). This mass loss is related to the dehydroxylation of the Cu-Ca-Al-LDH laminates and the formation of copper, calcium, and aluminum oxides. The Cu-Ca-Al-LDH exhibited a total mass loss of 29.0%. In the case of LDH-ITA, when the temperature was increased to near 200 °C, decomposition of itaconic acid began. The mass loss of LDH-ITA is considerably

higher than that of the unmodified Cu-Ca-Al-LDH. The LDH-ITA showed a total mass loss of 40.0% from 30 to 800 °C.

The FESEM images of the prepared Cu-Ca-Al-LDH and LDH-ITA are shown in Fig. 3 at three magnifications. The plate-like morphology of both Cu-Ca-Al-LDH and LDH-ITA crystallites is observable in the images. They exhibited a lamellar structure with sharp edges [38]. Also, the prepared Cu-Ca-Al-LDH shows more aggregation in comparison with modified LDH (LDH-ITA). This may be due to the formation of hydrogen bonds on the surface of the Cu-Ca-Al-LDH. In the case of LDH-ITA, the degree of reunion is reduced, and the particle size decreased [36].

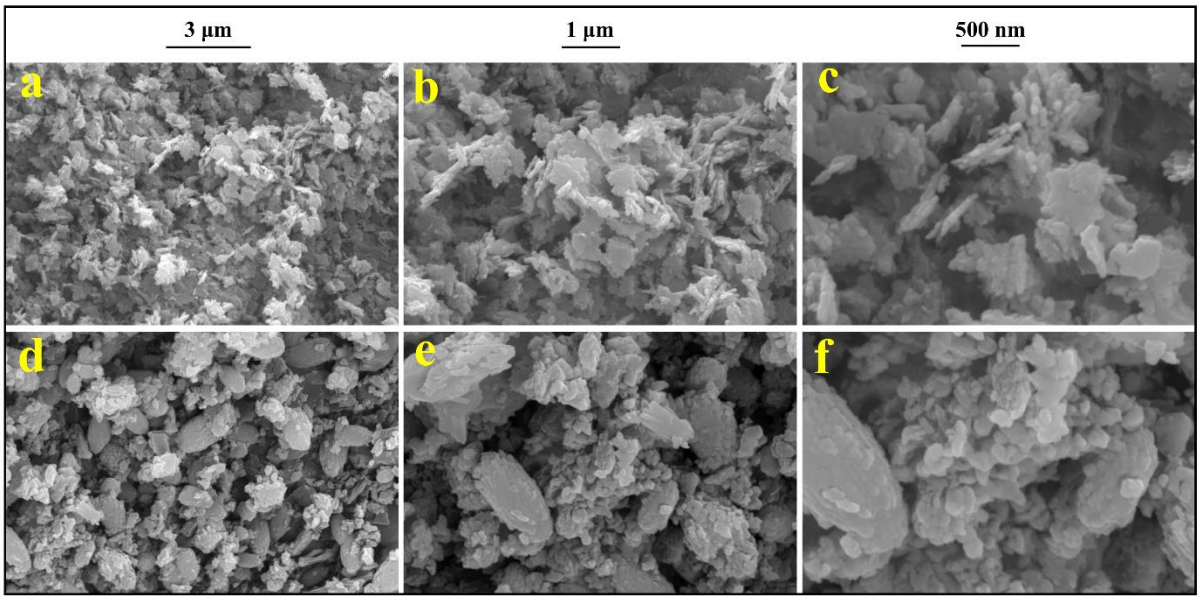

Figure 3. The scanning electron micrographs of the prepared Cu-Ca-Al-LDH (a-c) and LDH-ITA (d-f) with different magnifications.

The N_2 adsorption/desorption isotherms of the prepared Cu-Ca-Al-LDH and LDH-ITA are shown in Fig. 4. As can be seen in Fig. 4, Cu-Ca-Al-LDH showed a combination of type III and IV isotherms with H3-type hysteresis loops according to the IUPAC classification. The LDH-ITA exhibited IV type isotherm with H3-type hysteresis loops. The calculated parameters are shown in Table 1. The prepared Cu-Ca-Al-LDH showed a BET surface area of 15.6 m^2 g^{-1} while LDH-ITA exhibited a BET surface area of 24.8 m^2 g^{-1}. Also, pore

volumes of 0.142 and 0.080 cm^3 g^{-1} were obtained for Cu-Ca-Al-LDH and LDH-ITA, respectively.

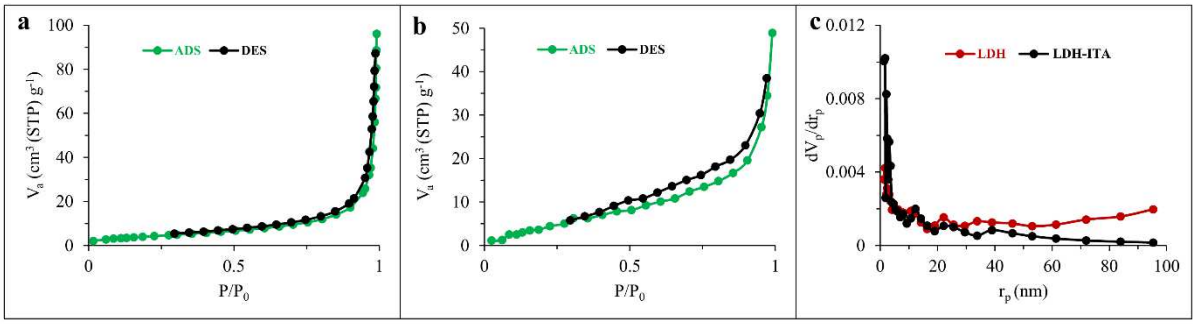

Figure 4. The N2 adsorption/desorption isotherms of Cu-Ca-Al-LDH (a), LDH-ITA (b), and the BJH pore size distribution curves of the samples (c).

Table 1. Textural properties of the synthesized materials.

Sample	BET	BJH	
	Surface area (m^2 g^{-1})	V_p (cm^3 g^{-1})	r_p (nm)
LDH	15.6	0.142	1.64
LDH-ITA	24.8	0.080	1.64

3.2. Adsorption studies

3.2.1. The effect of pH on adsorption

To study the effect of sample solution pH on the adsorption of Congo red onto the Cu-Ca-Al-LDH and LDH-ITA adsorbents, sample solution pHs between 5.0 and 9.0 were investigated. This range was selected due to the instability of Congo red below pH 5 [28]. All the experiments were done using 5 mL of an aqueous sample solution containing 50 mg L^{-1} of Congo red with the adsorbent dosage of 10.0 mg. The adsorption was performed at 298 K for 3 h with the help of magnetic stirring at 1500 rpm. After the adsorption procedure, the adsorbent was separated from the sample solution utilizing centrifugation (6000 rpm, 10 min) and the concentration of remained dye in the sample solution was determined using UV-Vis spectroscopy. The data are shown in Fig. 5a. As can be seen in Fig. 5a, with increasing

solution pH from 5.0 to 9.0, a continuous decrease in the removal efficiency of the two adsorbents was observed. The decrease in the Congo red removal efficiency is may be due to that the surface of the adsorbents becomes highly negative when pH increased from 5.0 to 9.0. The negative charge on the surface of the adsorbents results in electrostatically repelling of negatively charged Congo red [28]. Accordingly, pH=5.0 was selected for further experiments.

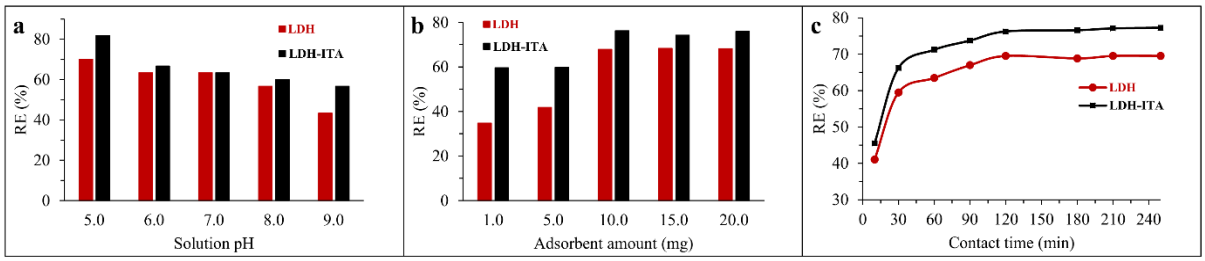

Figure 5. The effect of pH (a), adsorbent amount (b), and contact time (c) on the adsorption of Congo red by the prepared adsorbents**.**

3.2.2. The effect of the adsorbent amount

The effect of adsorbent amount on the adsorption of Congo red onto the Cu-Ca-Al-LDH, and LDH-ITA was studied in the range of 1.0-20.0 mg. In these experiments, 5 mL of a standard aqueous solution of Congo red at the concentration level of 50 mg L^{-1} (pH=5.0) was used. The experiments were performed at 298 K for 3 h with the help of magnetic stirring at 1500 rpm. After separation of the adsorbent from the sample solution (centrifugation at 6000 rpm for 10 min), the concentration of remained dye in the sample solution was determined using UV-Vis spectroscopy. As can be seen in Fig. 5b, the removal efficiency for two adsorbents was enhanced by enhancing the adsorbent amount from 1.0 to 10.0 mg and no further enhancement in removal efficiency was observed for higher adsorbent amounts. Based on the results, 10.0 mg of each of the adsorbents were selected as the adsorbent amount for further experiments.

295

296 *3.2.3. The effect of contact time*

297 To study the effect of contact time on the adsorption of Congo red onto the Cu-Ca-Al-
298 LDH and LDH-ITA adsorbents, various contact times between 10-250 min were investigated.
299 In the experiments, 5 mL of a standard solution of Congo red at the concentration level of 50
300 mg L^{-1} (pH=5.0) with an adsorbent dosage of 10.0 mg was used. The adsorption was
301 performed at 298 K. After separation of the adsorbent from the sample solution
302 (centrifugation at 6000 rpm for 10 min), the concentration of the remained dye in the sample
303 solution was determined. Figure 5c shows the effect of contact time on Congo red removal by
304 the prepared adsorbents. A remarkable enhancement in removal efficiency was observed for
305 the two adsorbents when contact time was increased from 10 to 120 min. Longer times had
306 no significant effect on the adsorption efficiency. The obtained data revealed a relatively fast
307 adsorption process. The high accessible sites of the adsorbents are mainly responsible for this
308 fast adsorption. Based on the results, a contact time of 120 min was used for further
309 experiments to ensure that equilibrium is reached.

310

311 *3.2.4. The adsorption kinetic studies*

312 To better understanding and study the mechanism of adsorption, kinetic studies were
313 conducted. The kinetic models of pseudo-first-order (PFO), pseudo-second-order (PSO),
314 Elovich, and intra-particle diffusion (IPD) were studied. The used equations are expressed in
315 the following equations:

316 $$\log(q_e - q_t) = \log q_e - \frac{k_1}{2.303} t \qquad (3)$$

317 $$\frac{t}{q_t} = \frac{1}{h} + \frac{1}{q_e} t \qquad (4)$$

318 $$h = k_2 \times q_e^2 \qquad (5)$$

$$q_t = \frac{\ln(\alpha\beta)}{\beta} + \frac{\ln t}{\beta} \quad (6)$$

$$q_t = k_{dif}(t)^{0.5} + C \quad (7)$$

In these equations, q_e (mg g^{-1}), q_t (mg g^{-1}), k_1 (min^{-1}), h (mg g^{-1} min^{-1}), k_2 (g mg^{-1} min^{-1}), α (mg g^{-1} min^{-1}) & β (g mg^{-1}), k_{dif} (mg g^{-1} min$^{-0.5}$), and C (mg g^{-1}) are the adsorption capacity at equilibrium, the adsorption capacity at time t, PFO rate constant, the initial sorption rate in PSO model, PSO rate constant, Elovich constants, IPD rate constant, and a constant, respectively. The results of the fitting are shown in Fig. 6 and Table 2. Data showed that, for both adsorbents, the PSO kinetic model provided better R^2 values than those obtained by other models. Accordingly, the physiochemical adsorption process can be well described with the PSO model.

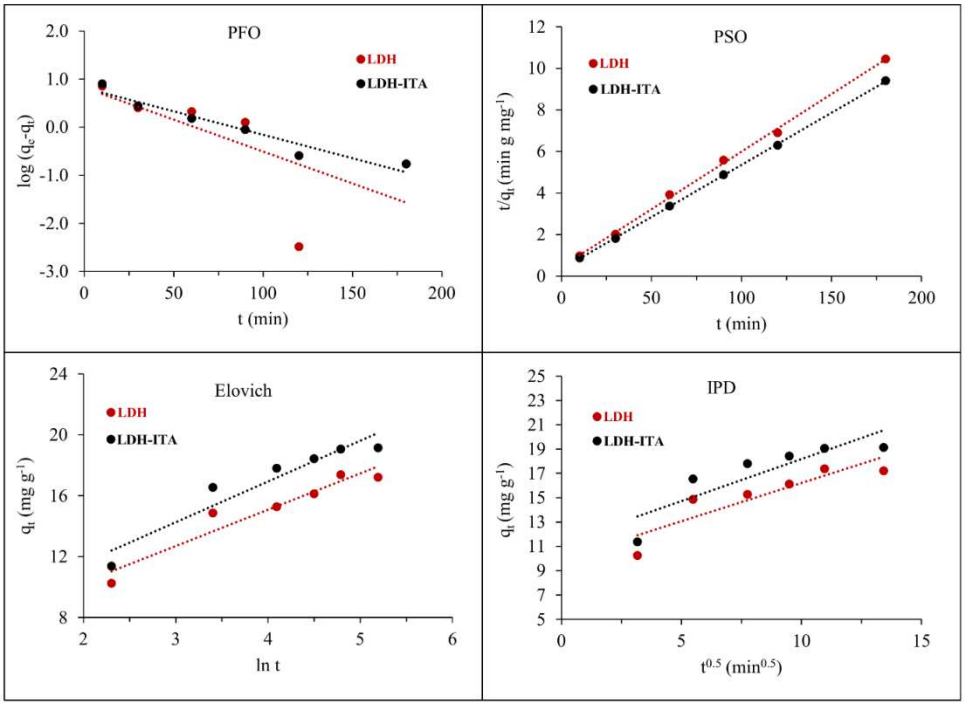

Figure 6. The kinetic adsorption models of pseudo-first-order (PFO), pseudo-second-order (PSO), Elovich, and intra-particle diffusion (IPD) for adsorption of Congo red by the prepared adsorbents.

334 **Table 2.** Parameters obtained by kinetic models for the adsorption of Congo red
335 onto LDH and LDH-ITA.

Model	Adsorbent	R^2	Parameters[a]		
PFO	LDH	0.4668	k_1 = 0.0306	q_e = 6.6	
	LDH-ITA	0.9347	k_1 = 0.0223	q_e = 6.5	
PSO	LDH	0.9985	k_2 = 0.0068	q_e = 18.0	h = 2.227
	LDH-ITA	0.9998	k_2 = 0.0073	q_e = 20.0	h = 2.890
Elovich	LDH	0.9186	α = 24.26	β = 0.4190	
	LDH-ITA	0.9106	α = 27.64	β = 0.3740	
IPD	LDH	0.7977	k_{dif} = 0.6283	C = 9.93	
	LDH-ITA	0.7623	k_{dif} = 0.6911	C =11.28	

[a] The units are as same as mentioned in section 3.2.4.

336

337

338 *3.2.5. The effect of Congo red concentration and adsorption isotherm*

339

340 To study the effect of Congo red initial concentration, concentrations between 10 and
341 300 mg L^{-1} (pH=5.0) were studied. An adsorbent dosage of 10.0 mg was applied and the
342 adsorption time was set to 120 min. The obtained data are shown in Fig. 7a. Maximum
343 adsorption capacities of 81 and 84 mg g^{-1} were obtained using Cu-Ca-Al-LDH and LDH-ITA
344 adsorbents, respectively. To study the equilibrium adsorption, Langmuir, Freundlich, and
345 Dubinin-Radushkevich (D-R) isotherm models were investigated. The equations of the linear
346 forms of the applied isotherm models are as follows:

347 $$\frac{C_e}{q_e} = \frac{1}{q_{max} \times k_L} + \frac{C_e}{q_{max}} \quad (8)$$

348 $$\log q_e = \frac{1}{n} \log C_e + \log k_F \quad (9)$$

349 $$\ln q_e = \ln q_{max} - B\,(RT \ln(1 + \frac{1}{C_e}))^2 \quad (10)$$

350 In these equations, C_e (mg L^{-1}), q_e (mg g^{-1}), q_{max} (mg g^{-1}), k_L (L mg^{-1}), n & k_F ((mg g^{-1})
351 (L $mg^{-1})^{1/n}$), B (mol^2 kJ^{-2}), R (j mol^{-1} K^{-1}), and T (K) are the concentration of Congo red at

equilibrium, adsorption capacity at equilibrium, the maximum adsorption capacity of adsorbent, the Langmuir constant, the Freundlich isotherm constants for adsorption capacity and adsorption intensity, the Dubinin–Radushkevich isotherm constant, the universal gas constant, and temperature, respectively. Figure 7 and Table 3 show the adsorption isotherms and the calculated parameters. Considering the R^2 value, the Freundlich model showed the best fit with the experimental data obtained by both adsorbents. The R^2 values of the Freundlich model were obtained 0.9411 and 0.9320 for Cu-Ca-Al-LDH and LDH-ITA adsorbents, respectively. The Freundlich adsorption isotherm model representing multilayer, heterogeneous adsorption sites.

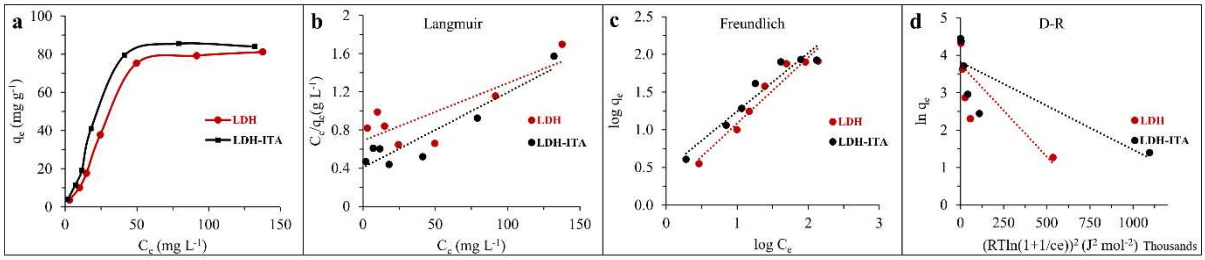

Figure 7. The equilibrium isotherm (a) and the isotherm models of Langmuir (b), Freundlich (c), and Dubinin–Radushkevich (d) for adsorption of Congo red by the prepared adsorbents.

Table 3 The parameters obtained by isotherm models for the adsorption of Congo red onto LDH and LDH-ITA.

Model	Adsorbent	R^2	Parameters[a]	
Langmuir	LDH	0.6805	$k_L = 0.0087$	$q_{max} = 166.6$
	LDH-ITA	0.8782	$k_L = 0.0194$	$q_{max} = 126.6$
Freundlich	LDH	0.9411	$k_F = 1.620$	$n = 1.142$
	LDH-ITA	0.9320	$k_F = 2.945$	$n = 1.289$
D-R	LDH	0.6479	$B = 4.93 \times 10^{-6}$	$q_{max} = 42.5$
	LDH-ITA	0.6450	$B = 2.34 \times 10^{-6}$	$q_{max} = 45.6$

[a] The units are as same as mentioned in section 3.2.5.

3.3. Comparison study

Contact time (equilibrium time) and adsorption capacity are two important factors in the adsorption process of an adsorbate species by an adsorbent material. The shorter and higher

the adsorption time and the adsorbent capacity, respectively, the more efficient the adsorption process. Table 4 compares the adsorption capacities of several adsorbents as well as corresponding optimal adsorption conditions. As shown in Table 4, the highest adsorption capacities were observed at acidic pHs for all adsorbents. Also, compared to the adsorbents reported in Table 4, adsorbents synthesized in this work have a shorter adsorption time and a higher adsorption capacity, which indicates the acceptable performance of these adsorbents. One possible reason for observing this acceptable performance is the adsorption mechanism, which occurs in both anion exchange and surface adsorption by H-bonding pathway as depicted in Scheme 1.

Table 4. Comparison of a maximum adsorption capacities of Cu-Ca-Al-LDH and LDH-ITA for removal of Congo red dye by various reported adsorbents.

Adsorbents[a]	q_{ma} (mg g^{-1})	pH	Equilibrium time (min)	Ref.
Cu-Ca-Al-LDH	81	5.0	120	This work
LDH-ITA	84	5.0	120	This work
AuNPs-coated AC	71	6.5	270	[41]
AgNPs-coated AC	64	6.5	270	[41]
*p*TSA-Pani@GO-CNT	66	5.0	300	[42]
Neem leaf powder	41	6.7	300	[43]
hollow $ZnFe_2O_4$ microspheres	16	6.0	120	[44]
Aspergillus niger biomass	14	6.0	1800	[45]

[a]NPs: nanoparticles; AC: activated carbon; *p*TSA: para toluene sulfonic acid; Pani: polyaniline; GO: graphene oxide; CNT: multiwalled carbon nanotube.

4. Conclusions

In conclusion, Cu-Ca-Al/NO_3-LDH was functionalized with itaconic acid. Water as an environmentally-friendly solvent was used in the synthesis procedures. The prepared materials were applied as novel adsorbents for adsorption purposes. The newly prepared materials showed good performance toward Congo red removal from aqueous solutions. The effect of experimental parameters (sample solution pH, adsorbent dosage, contact time, and initial concentration of the dye) was studied. The kinetic studies showed that the best fit was

achieved with the pseudo-second-order model for the adsorption of Congo red using the two prepared adsorbents. Three isotherm models were used to investigate the equilibrium adsorption studies. The data showed that the Freundlich model showed the best fit with R^2 values of 0.9411 and 0.9320 for Cu-Ca-Al-LDH and LDH-ITA adsorbents, respectively. Maximum adsorption capacities of 81 and 84 mg g^{-1} were obtained using Cu-Ca-Al-LDH and LDH-ITA adsorbents, respectively. Finally, the prepared adsorbents showed acceptable characteristics to be considered as effective adsorbents for anionic dye (e.g. Congo red) removal from aqueous media.

Conflict of interest

The authors declare no competing financial interest.

Acknowledgment

The authors wish to thank the research council of the Isfahan University of Technology.

References

[1] Z. Babaei, A.N. Chermahini, M. Dinari, M. Saraji, A. Shahvar, A sulfonated triazine-based covalent organic polymer supported on a mesoporous material: a new and robust material for the production of 5-hydroxymethylfurfural, Sustainable Energy & Fuels, 3, 1024-1032 (2019).

[2] A. Shahzeydi, M. Ghiaci, H. Farrokhpour, A. Shahvar, M. Sun, M. Saraji, Facile and green synthesis of copper nanoparticles loaded on the amorphous carbon nitride for the oxidation of cyclohexane, Chemical Engineering Journal, 370, 1310-1321 (2019).

[3] M. Rezaie, M. Dinari, A.N. Chermahini, M. Saraji, A. Shahvar, Preparation of kapa carrageenan-based acidic heterogeneous catalyst for conversion of sugars to high-value added materials, International Journal of Biological Macromolecules, 165, 1129-1138 (2020).

[4] Q. Zhang, E. Uchaker, S.L. Candelaria, G. Cao, Nanomaterials for energy conversion and storage, Chemical Society Reviews, 42, 3127-3171 (2013).

[5] K. Pyrzynska, Use of nanomaterials in sample preparation, TrAC Trends in Analytical Chemistry, 43, 100-108 (2013).

[6] M. Ahmadi, H. Elmongy, T. Madrakian, M. Abdel-Rehim, Nanomaterials as sorbents for sample preparation in bioanalysis: A review, Analytica Chimica Acta, 958, 1-21 (2017).

[7] A. Shahvar, R. Soltani, M. Saraji, M. Dinari, S. Alijani, Covalent triazine-based framework for micro solid-phase extraction of parabens, Journal of Chromatography A, 1565, 48-56 (2018).

[8] M. Saraji, A. Shahvar, Metal-organic aerogel as a coating for solid-phase microextraction, Analytica Chimica Acta, 973, 51-58 (2017).

[9] S. Zhao, X. Fan, J. Yang, H. Huang, C. Xia, R. Jing, M. Wu, Z. Zhang, A. Liu, Q. Zhang, Z. Enhanced removal of Cr(VI) from wastewater by nanoscale zero valent iron supported on layered double hydroxides, Journal of Porous Materials 27, 1701–1710 (2020).

[10] M. Dinari, N. Roghani, Calcium Iron Layered Double Hydroxide/Poly(vinyl chloride) Nanocomposites: Synthesis, Characterization and Cd2+ Removal Behavior, Journal of Inorganic and Organometallic Polymers and Materials, 30, 808–819 (2020).

[11] J. Imanipoor, A. Ghafelebashi, M. Mohammadi, M. Dinari, M.R. Ehsani, Fast and effective adsorption of amoxicillin from aqueous solutions by L-methionine modified montmorillonite K10, Colloids and Surfaces A:, 611, 125792 (2021).

[12] E. S. Behbahani, K. Dashtian, M. Ghaedi, Fe/Co-chalcogenide-stabilized Fe3O4 nanoparticles supported MgAl-layered double hydroxide as a new magnetically separable sorbent for the simultaneous spectrophotometric determination of anionic dyes, Microchemical Journal, 152, 104431 (2020).

[13] M. Dinari, S. Neamati, Surface modified layered double hydroxide/polyaniline nanocomposites: Synthesis, characterization and Pb^{2+} removal, Colloids and Surfaces A:, 598, 124438 (2020).

[14] M. Dinari, R. Soltani, G. Mohammadnezhad, Kinetics and thermodynamic study on novel modified–mesoporous silica MCM-41/polymer matrix nanocomposites: effective adsorbents for trace CrVI removal, Journal of Chemical & Engineering Data, 62, 2316-2329 (2017).

[15] R. Soltani, A. Shahvar, H. Gordan, M. Dinari, M. Saraji, Covalent triazine framework-decorated phenyl-functionalised SBA-15: its synthesis and application as a novel nanoporous adsorbent, New Journal of Chemistry, 43, 13058-13067 (2019).

[16] K.-H. Goh, T.-T. Lim, Z. Dong, Application of layered double hydroxides for removal of oxyanions: a review, Water research, 42, 1343-1368 (2008).

[17] A. Mokhtar, S. Abdelkrim, F. Zaoui, M. Sassi, B. Boukoussa, Improved Stability of Starch@Layered-Materials Composite Films for Methylene Blue Dye Adsorption in Aqueous Solution, Journal of Inorganic and Organometallic Polymers and Materials, 29, 1807–1817 (2019).

[18] J. He, M. Wei, B. Li, Y. Kang, D.G. Evans, X. Duan, Preparation of layered double hydroxides, in: Layered double hydroxides, Springer, pp. 89-119 (2006).

[19] X. Duan, D.G. Evans, Layered double hydroxides, Springer Science & Business Media, 2006.

[20] H. Nabipour, Controlled release of Diclofenac, an anti-inflammatory drug by nanocompositing with layered zinc hydroxide, Journal of Inorganic and Organometallic Polymers and Materials, 30, 3826–3831 (2020).

[21] G. Fan, F. Li, D.G. Evans, X. Duan, Catalytic applications of layered double hydroxides: recent advances and perspectives, Chemical Society Reviews, 43, 7040-7066 (2014).

460 [22] X. Long, Z. Wang, S. Xiao, Y. An, S. Yang, Transition metal based layered double hydroxides
461 tailored for energy conversion and storage, Materials today, 19, 213-226 (2016).
462 [23] H. Pang, Y. Wu, X. Wang, B. Hu, X. Wang, Recent advances in composites of graphene and
463 layered double hydroxides for water remediation: a review, Chemistry–An Asian Journal, 14, 2542-
464 2552 (2019).
465 [24] M. Zubair, M. Daud, G. McKay, F. Shehzad, M.A. Al-Harthi, Recent progress in layered double
466 hydroxides (LDH)-containing hybrids as adsorbents for water remediation, Applied Clay Science,
467 143, 279-292 (2017).
468 [25] H. Wang, X. Li, J. Ma, Q. Jia, Facile synthesis of polymer monolith functionalized with layered
469 double hydroxide as effective preconcentration materials for fluorescent whitening agents,
470 Microchemical Journal, 132, 1071-1077 (2017).
471 [26] R. Soltani, A. Shahvar, M. Dinari, M. Saraji, Environmentally-friendly and ultrasonic-assisted
472 preparation of two-dimensional ultrathin Ni/Co-NO_3 layered double hydroxide nanosheet for micro
473 solid-phase extraction of phenolic acids from fruit juices, Ultrasonics Sonochemistry, 40, 395-401
474 (2018).
475 [27] M. Laipan, J. Yu, R. Zhu, J. Zhu, A.T. Smith, H. He, D. O'Hare, L. Sun, Functionalized layered
476 double hydroxides for innovative applications, Materials Horizons, 7, 715-745 (2020).
477 [28] G. Sriram, U. Uthappa, D. Losic, M. Kigga, H.-Y. Jung, M.D. Kurkuri, Mg–Al-Layered Double
478 Hydroxide (LDH) Modified Diatoms for Highly Efficient Removal of Congo Red from Aqueous
479 Solution, Applied Sciences, 10, 2285 (2020).
480 [29] N. Asses, L. Ayed, N. Hkiri, M. Hamdi, Congo red decolorization and detoxification by
481 Aspergillus niger: removal mechanisms and dye degradation pathway, BioMed research international,
482 2018 (2018).
483 [30] A. Tkaczyk, K. Mitrowska, A. Posyniak, Synthetic organic dyes as contaminants of the aquatic
484 environment and their implications for ecosystems: A review, Science of The Total Environment,
485 717, 137222 (2020).
486 [31] Y. Zhou, J. Lu, Y. Zhou, Y. Liu, Recent advances for dyes removal using novel adsorbents: a
487 review, Environmental pollution, 252, 352-365 (2019).

488 [32] T. Ngulube, J.R. Gumbo, V. Masindi, A. Maity, An update on synthetic dyes adsorption onto
489 clay based minerals: A state-of-art review, Journal of environmental management, 191 (2017) 35-57.
490 [33] V. Gupta, Application of low-cost adsorbents for dye removal–a review, Journal of
491 environmental management, 90, 2313-2342 (2009).
492 [34] H. Yi, S. Zhao, X. Tang, P. Ning, H. Wang, D. He, Influence of calcination temperature on the
493 hydrolysis of carbonyl sulfide over hydrotalcite-derived Zn–Ni–Al catalyst, Catalysis
494 Communications, 12, 1492-1495 (2011).
495 [35] R. Lafi, K. Charradi, M.A. Djebbi, A.B.H. Amara, A. Hafiane, Adsorption study of Congo red
496 dye from aqueous solution to Mg–Al–layered double hydroxide, Advanced Powder Technology, 27,
497 232-237 (2016).
498 [36] S. Wang, X. Yang, F. Wang, Z. Song, H. Dong, L. Cui, Effect of Modified Hydrotalcites on
499 Flame Retardancy and Physical Properties of Paper, BioResources, 14, 3991-4005 (2019).
500 [37] Y. Shi, F. Chen, J. Yang, M. Zhong, Crystallinity and thermal stability of LDH/polypropylene
501 nanocomposites, Applied Clay Science, 50, 87-91 (2010).
502 [38] G. Geng, R. Wei, T. Liang, M. Zhou, G. Xiao, Hydrogenolysis of glycerol to propanediols on
503 Cu–Ca–Al hydrotalcites derived catalysts, Reaction Kinetics, Mechanisms and Catalysis, 117, 239-
504 251 (2016).
505 [39] J. Ashok, Y. Kathiraser, M. Ang, S. Kawi, Bi-functional hydrotalcite-derived NiO–CaO–Al_2O_3
506 catalysts for steam reforming of biomass and/or tar model compound at low steam-to-carbon
507 conditions, Applied Catalysis B: Environmental, 172, 116-128 (2015).
508 [40] P.H. Chang, Y.P. Chang, S.Y. Chen, C.T. Yu, Y.P. Chyou, Ca-rich Ca–Al-oxide, high-
509 temperature-stable sorbents prepared from hydrotalcite precursors: synthesis, characterization, and
510 CO_2 capture capacity, ChemSusChem, 4, 1844-1851 (2011).
511 [41] J. Pal, M.K. Deb, Efficient adsorption of congo red dye from aqueous solution using green
512 synthesized coinage nanoparticles coated activated carbon beads, Applied Nanoscience, 4, 967-978
513 (2014).

[42] M.O. Ansari, R. Kumar, S.A. Ansari, S.P. Ansari, M. Barakat, A. Alshahrie, M.H. Cho, Anion selective pTSA doped polyaniline@graphene oxide-multiwalled carbon nanotube composite for Cr (VI) and Congo red adsorption, Journal of colloid and interface science, 496, 407-415 (2017).

[43] K.G. Bhattacharyya, A. Sharma, Azadirachta indica leaf powder as an effective biosorbent for dyes: a case study with aqueous Congo Red solutions, Journal of Environmental Management, 71, 217-229 (2004).

[44] R. Rahimi, H. Kerdari, M. Rabbani, M. Shafiee, Synthesis, characterization and adsorbing properties of hollow Zn-Fe_2O_4 nanospheres on removal of Congo red from aqueous solution, Desalination, 280, 412-418 (2011).

[45] Y. Fu, T. Viraraghavan, Removal of Congo Red from an aqueous solution by fungus Aspergillus niger, Advances in Environmental Research, 7, 239-247 (2002).

Figures caption

Fig. 1. The FT-IR spectra of the prepared Cu-Ca-Al-LDH and LDH-ITA.

Fig. 2. The XRD patterns (a) and the TGA thermograms (b) of the prepared Cu-Ca-Al-LDH and LDH-ITA.

Fig. 3. The scanning electron micrographs of the prepared Cu-Ca-Al-LDH (a-c) and LDH-ITA (d-f) with different magnifications.

Fig. 4. The N_2 adsorption/desorption isotherms of Cu-Ca-Al-LDH (a), LDH-ITA (b), and the BJH pore size distribution curves of the samples (c).

Fig. 5. The effect of pH (a), adsorbent amount (b), and contact time (c) on the adsorption of Congo red by the prepared adsorbents.

Fig. 6. The kinetic adsorption models of pseudo-first-order (PFO), pseudo-second-order (PSO), Elovich, and intra-particle diffusion (IPD) for adsorption of Congo red by the prepared adsorbents.

Fig. 7. The equilibrium isotherm (a) and the isotherm models of Langmuir (b), Freundlich (c), and Dubinin–Radushkevich (d) for adsorption of Congo red by the prepared adsorbents.

Figures

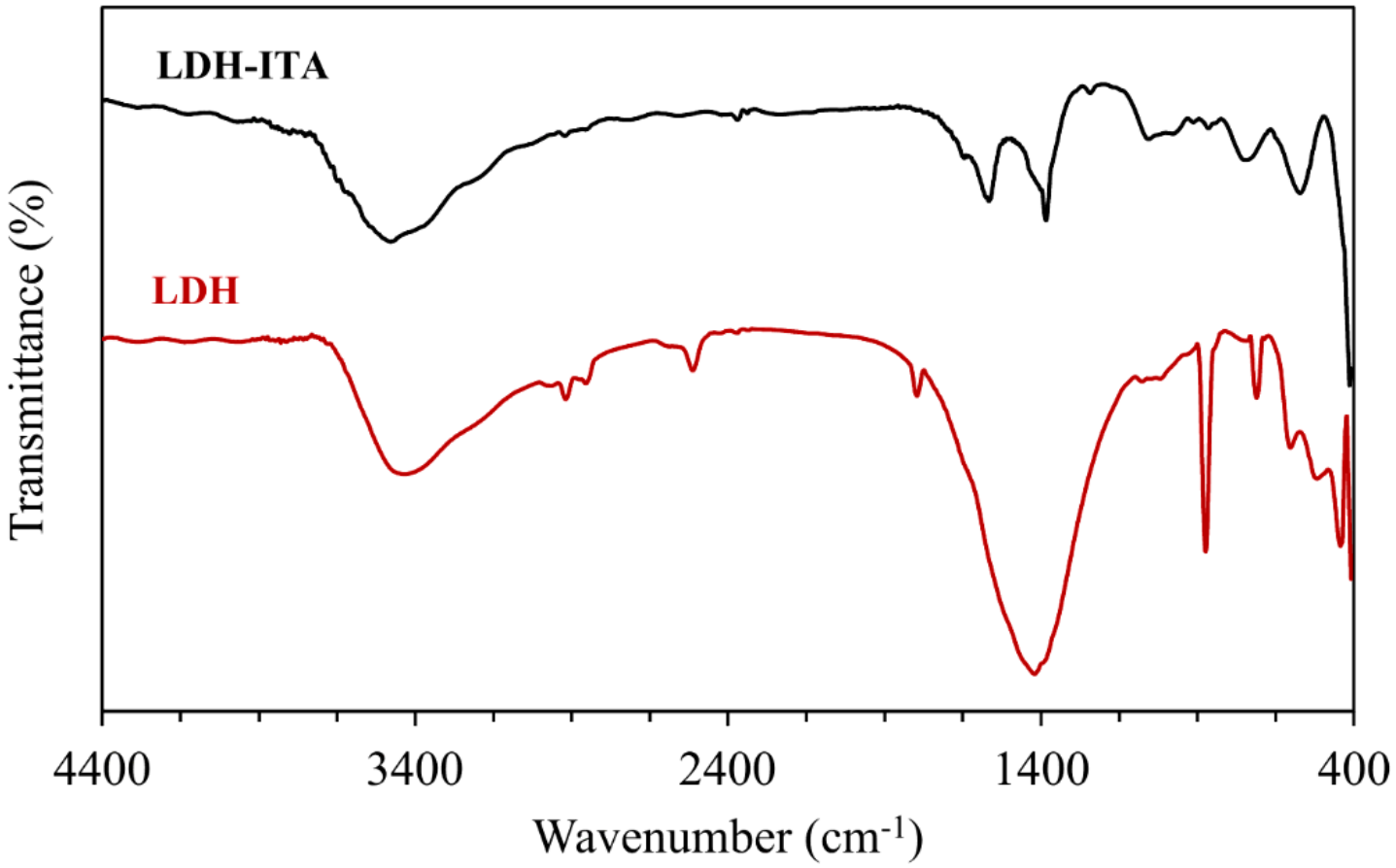

Figure 1

FT-IR spectra of the Cu-Ca-Al-LDH and LDH-ITA.

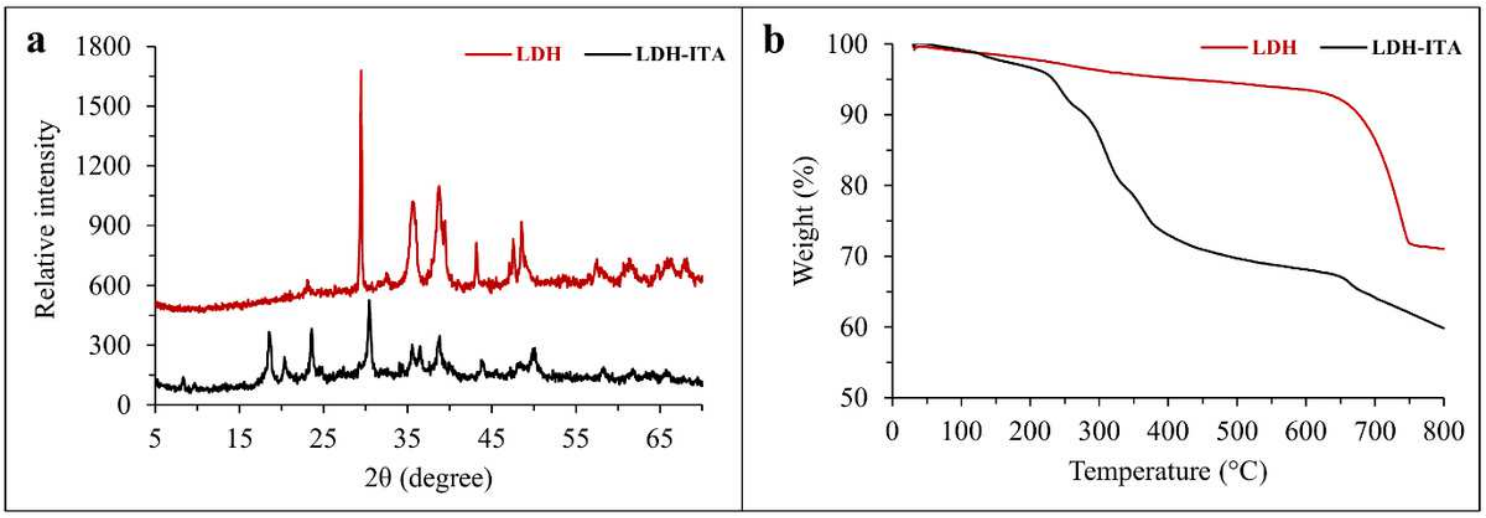

Figure 2

The XRD patterns (a) and the TGA thermograms (b) of the prepared Cu-Ca-Al-LDH and LDH-ITA.

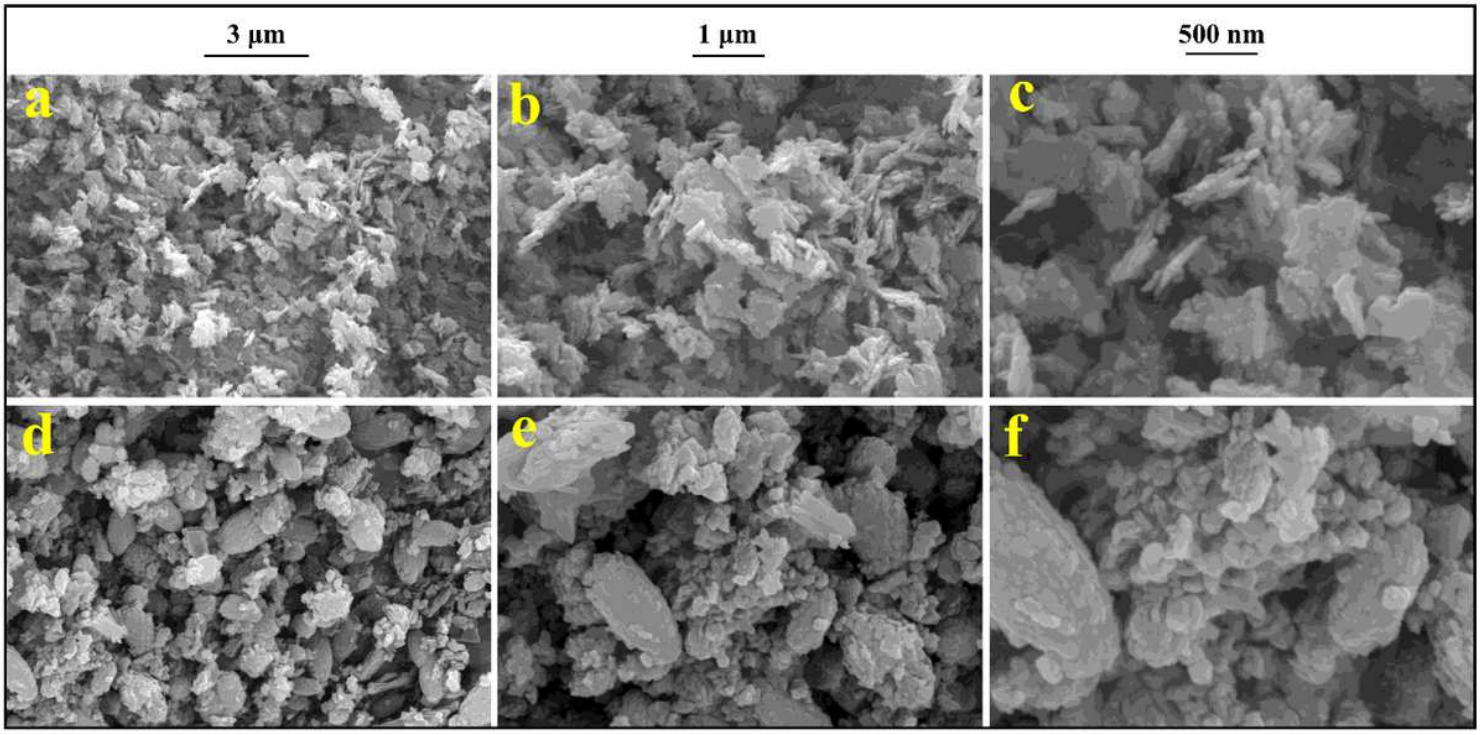

Figure 3

The scanning electron micrographs of the prepared Cu-Ca-Al-LDH (a-c) and LDH-ITA (d-f) with different magnifications.

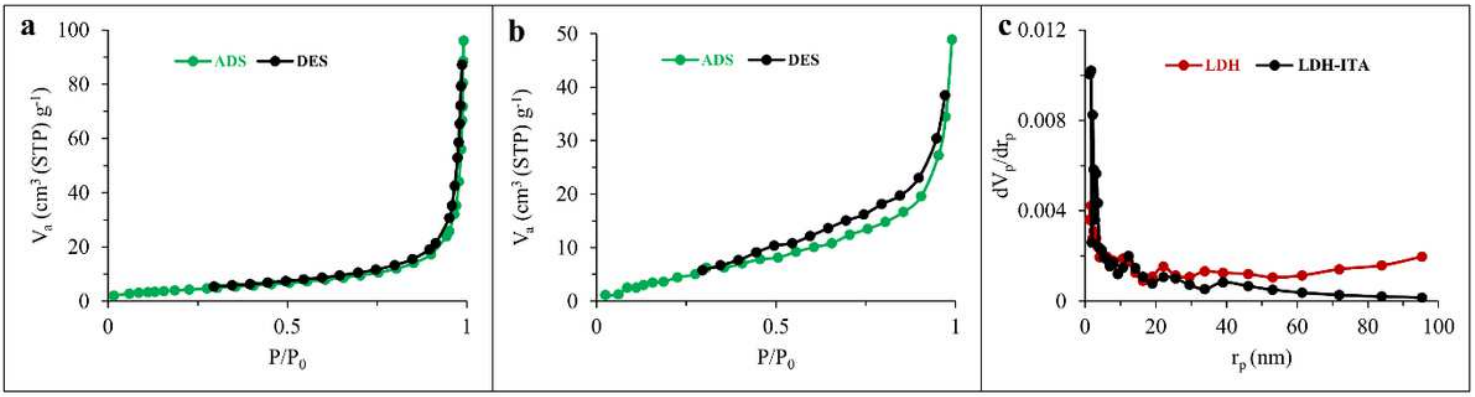

Figure 4

The N2 adsorption/desorption isotherms of Cu-Ca-Al-LDH (a), LDH-ITA (b), and the BJH pore size distribution curves of the samples (c).

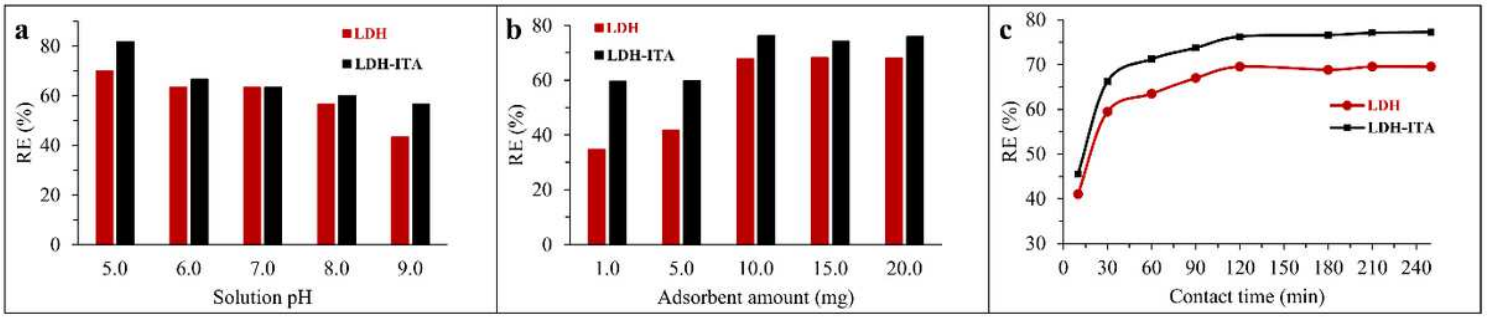

Figure 5

The effect of pH (a), adsorbent amount (b), and contact time (c) on the adsorption of Congo red by the prepared adsorbents.

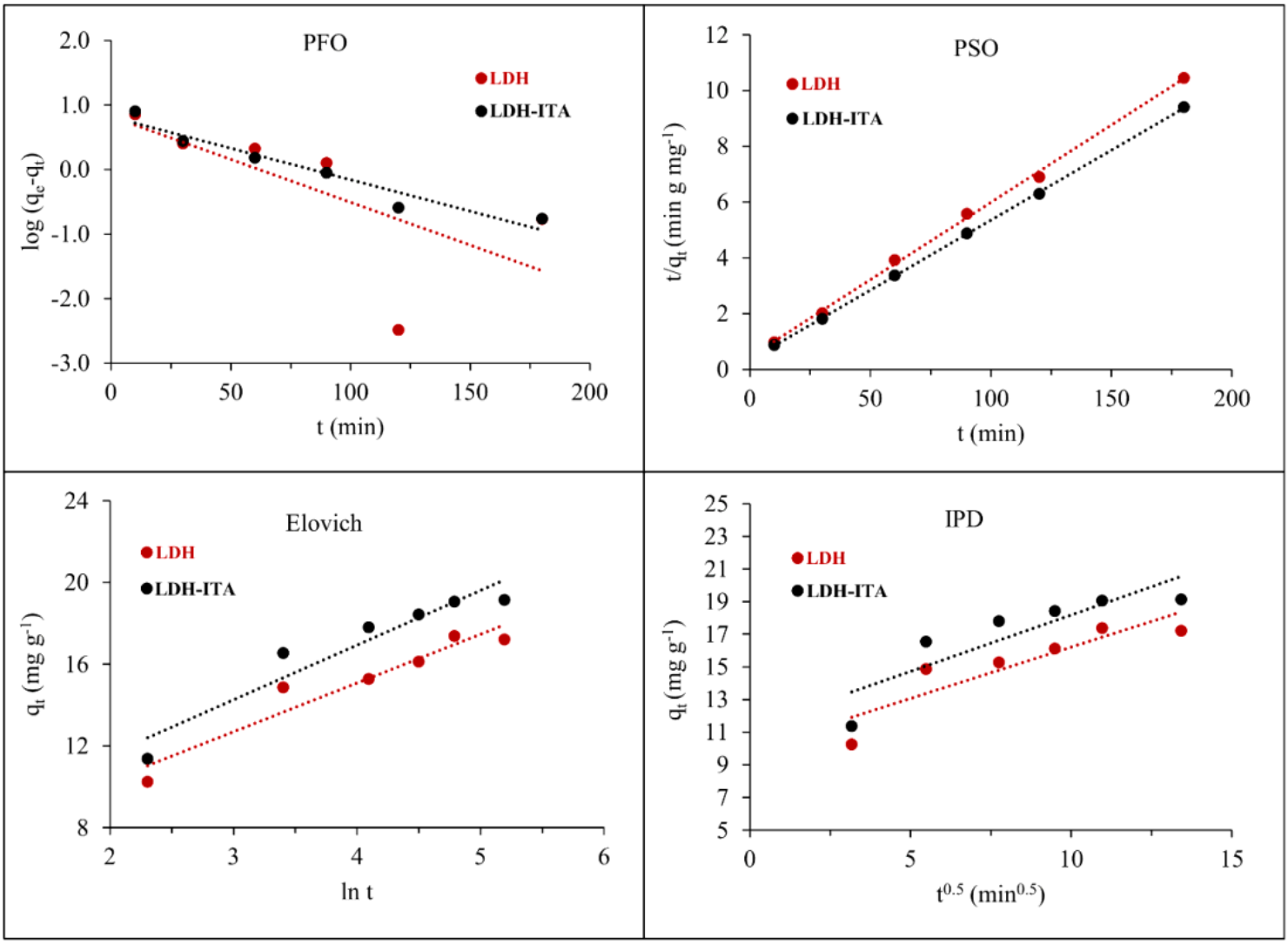

Figure 6

The kinetic adsorption models of pseudo-first-order (PFO), pseudo-second-order (PSO), Elovich, and intra-particle diffusion (IPD) for adsorption of Congo red by the prepared adsorbents.

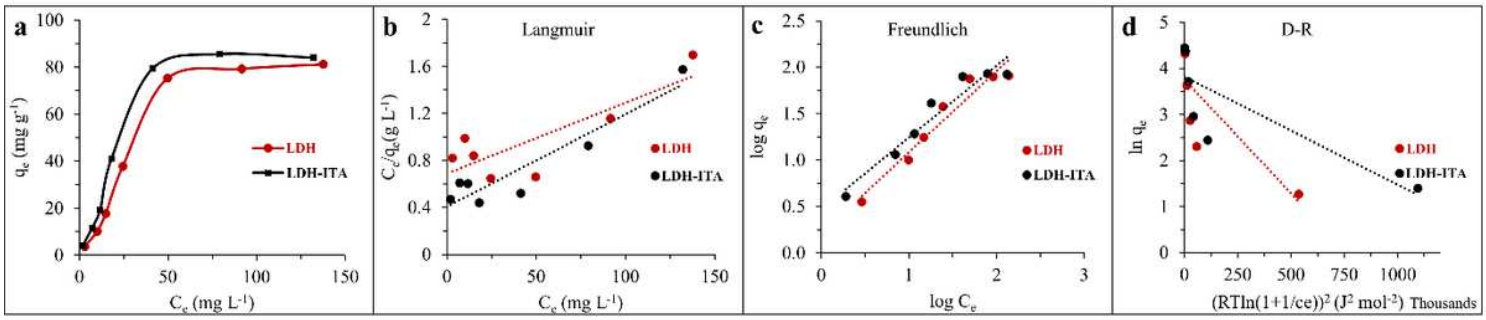

Figure 7

The equilibrium isotherm (a) and the isotherm models of Langmuir (b), Freundlich (c), and Dubinin–Radushkevich (d) for adsorption of Congo red by the prepared adsorbents.

Supplementary Files

This is a list of supplementary files associated with this preprint. Click to download.

- Scheme1.png